Gas hydrate characterization from acoustic impedance and porosity inversion in the northern Hikurangi margin, New Zealand from new drilling data of IODP 372

Uma Shankar
Department of Geophysics, Institute of Science, Banaras Hindu University, Varanasi-221005
Email: umashankar@bhu.ac.in

Keywords

Gas hydrate, BSR, acoustic impedance inversion, porosity inversion, Sonic log, density log and porosity log.

Summary

Presence of gas hydrate is identified on the seismic section by bottom simulating reflector (BSR), which is pressure and temperature dependent physical boundary between hydrate and water saturated or gas bearing sediments. High resolution multichannel seismic data used to delineate the BSRs in the Hikurangi margin, New Zealand. Simultaneously, identified BSR characterized using coring and well logging measurements from acoustic impedance inversion and porosity inversion. It is always a challenging task to get the acoustic impedance and porosity information away from well position at the prospective gas-hydrate occurrence zone. Acoustic impedance from model based acoustic impedance inversion and porosity values throughout the seismic profile by using the porosity inversion technique on the post-stack data was performed. Inverted acoustic impedance values ranges from ~3050 to ~3450 (m/s)*(g/cc) along seismic section at and above BSR. Below the BSR decreasing trend of inverted acoustic impedance in the range of ~2600 to ~2950 (m/s)*(g/cc) interpreted free gas zone. Inverted porosity along seismic section above BSR in the range of ~50% to ~60%, whereas the porosity value below the BSR in the free gas zone ranges from ~60% to ~70%. Comparatively low porosity and high acoustic impedance at the upper zone sediment saturated with gas hydrate and high porosity and low acoustic impedance in the lower zone sediment saturated with free gas separated by clear BSR.

Introduction

Gas hydrate occurrences are often inferred from seismic data through observations of a bottom-simulating reflector (BSR) having characteristic reverse polarity with respect to the seafloor reflection (Taylor et al., 2000; Shankar and Riedel, 2010). Additionally, a BSR often cross-cuts sedimentary reflections and is sub-parallel to the seafloor reflection on a regional scale. The BSR marks the boundary between gas hydrate bearing sediments above and free-gas-bearing sediments below. The presence of gas hydrate in marine sediments can significantly affect the bulk physical properties of the sediments. Presence of gas hydrates reveal relatively high P-wave wave velocity compared to pore-filling fluids such as water or gas (Stoll et al., 1971, Tucholke et al., 1977). Resistivity appears to be the most strongly affected by the presence of gas hydrate in the marine sediment. Its inclusion in the pore space of marine sediments can significantly increase the electrical resistivity of the sediment. The measurement of such properties can therefore be used to estimate gas hydrate saturation (Shankar and Riedel, 2011). Natural gas hydrate act as an insulator and stop electric conduction. Therefore, high electrical resistivity in gas hydrates bearing sediments. Gas hydrate formation in the sediments reduces the effective porosity. Resistivity logs data extensively used to characterize gas hydrate bearing sediments and estimation of gas hydrate saturations (Helgerud et al., 1999, Hyndman et al., 2001).

Hikurangi Margin is one of the most seismically active regions of the world where there are frequent Earthquakes, slow slip events, and submarine landslides occur that causing Tsunami and high tides. (Pecher et al., 2018) Many geoscientists published literature has given some hypothesis that these events are may be linked to the presence of gas hydrates and creep-like deformation. Also, gas hydrate considered as potential source of energy for future. Thus, this project is a means of identifying a gas hydrate reservoir precisely by using available seismic data and IODP-372 well-log data to know the nature and distribution of gas hydrate in Hikurangi margin. At the northern Hikurangi margin, the Pacific plate subducts beneath the Australian plate (eastern North Island, New Zealand) at a rate of 4.5–5.5 cm/year (Pecher et al., 2018) as shown in Figure 1. The oceanic subducting plate comprises the Hikurangi Plateau, a rough-crust, seamount-studded

Acoustic impedance inversion and porosity inversion

large igneous province of Cretaceous age (120–90 Ma).

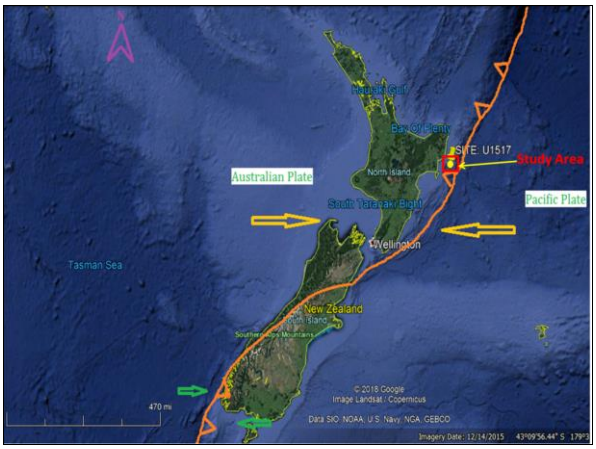

Figure 1. Drilling area and site location in the northern Hikurangi margin of New Zealand targeted during International Ocean Discovery Program (IODP) 372.

Identification of gas hydrate in the Hikurangi margin, New Zealand was inferred based on the BSR on seismic sections. Downhole logging and coring confirmed gas hydrate in the Hikurangi margin during International Ocean Discovery Program (IODP) Expedition 372 from 26th November 2017 to 4th January 2018. Multi-channel seismic data along Hikurangi margin shows major geomorphic features such as land slide, prominent BSR with opposite polarity with respect to seafloor, cross-cutting with dipping reflectors, and high reflectivity below the BSR (Fig. 2).

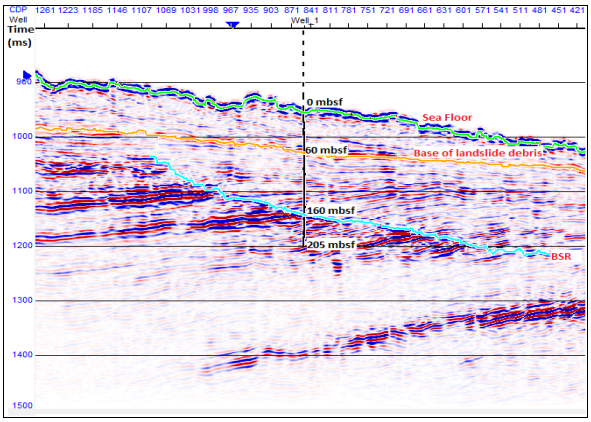

Figure 2: Seismic section from Hikurangi margin shows BSR parallel to the seafloor underlain by a high reflectivity zone.

Methods

Acoustic impedance (AI) inversion is the technique of getting layer property of the subsurface based on the reflectivity (R) data and the wavelet (W) from seismic data taking reference from the density and P-wave velocity log from well-log data. As this is the post-stack model-based inversion the seismic data are stacked at zero-offset so we take a single wavelet for inversion (first statistical and after well-to-seismic correlation, deterministic wavelet) has been used.

$$AI = \frac{Z_2 - Z_1}{Z_2 - Z_1} \quad \ldots\ldots (1)$$

Where, Z represents the product of density (ρ) and velocity (v). Whereas 2 and 1 subscripts are the underlying and overlying rock sediment layers respectively.

The seismic traces obtained from the seismic acquisition are the convolution of impulse (i.e. wavelet) with the reflectivity of the earth at different depth sequences according to the impedance of the seismic strata plus noises. Now, the inversion is the process to get the impedance information based on the recorded seismic data. The fundamental equation of convolution is shown in the following equation:

$S = W * R + Noise$……...(2)

However, we assume that our data is noise free and hence we neglect this noise term and thus the reflectivity obtained is:

$R = W^{-1} * S$……..…..(3)

This obtained reflectivity (interval property) is converted into impedance property (i.e. layer or rock property) as shown above from equation 1.

At first, the acoustic reflectivity (R_{AI}) and porosity reflectivity (R_φ) as defined by Rasmussen and Maver (1996) has been calculated.

$R_{AI} = ½ [\log (Z_{i+1}) - \log(Z_i)]$……...….(4)

where, Z_i = Acoustic impedance of the i^{th} layer ($\rho_i * v_i$). Similarly,

$$R_\varphi = ½ \left[\log \left(\frac{\varphi_{i+1}}{1-\varphi_{i+1}}\right) - \log \left(\frac{\varphi_{i+1}}{1-\varphi_i}\right)\right] \quad \ldots\ldots..\ldots\ldots (5)$$

where φ_i and φ_{i+1} are the porosity values of i^{th} and $(i+1)^{th}$ layers.

Acoustic impedance and porosity logs are used for estimation of wavelet and low frequency models. Therefore, porosity wavelet generated by multiplying the acoustic impedance wavelet (computed from density and velocity logs) with the

Acoustic impedance inversion and porosity inversion

correlation factor. The estimated wavelet and a low frequency model enable the execution of seismic inversion (Russell and Hampson, 1991). The estimated acoustic impedance and porosity reflectivity is showing a linear relation (Fig. 3)

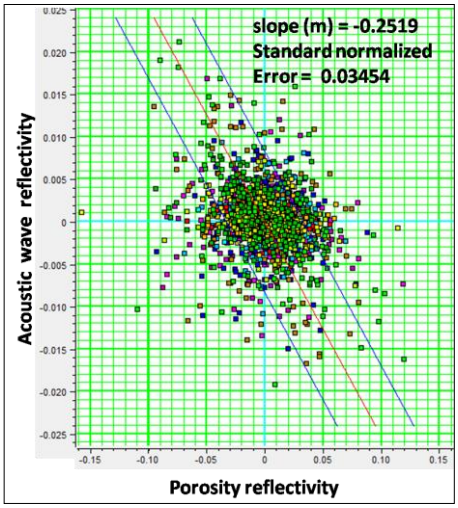

Figure 3: The crossplot of porosity reflectivity versus acoustic P-wave reflectivity showing near-linear trend.

Examples

In this study seismic and log data used for characterization of gas hydrate zone in the Hikurangi magin New Zealand. The seismic data sets of Hikurangi magin previously used for defining geophysical drilling targets and site selection for the IODP Expedition 372. BSR and BSR-like features are identified along available seismic lines followed by enhanced reflectivity zone (Fig. 2).

Base of gas hydrate stability (BGHS) is modeled using water depth, seafloor temperature, geothermal gradient, and gas and fluid compositions. Using an average velocity between seafloor and BSR, potential gas hydrate stability thickness estimated at Site U1517 in the Hikurangi margin is ~160 meter below seafloor (Fig. 4), which shows close correspondence with the observed BSR on seismic section. The BGHS depth predicted from the phase boundary modeling using geothermal gradients (~40°C/km),

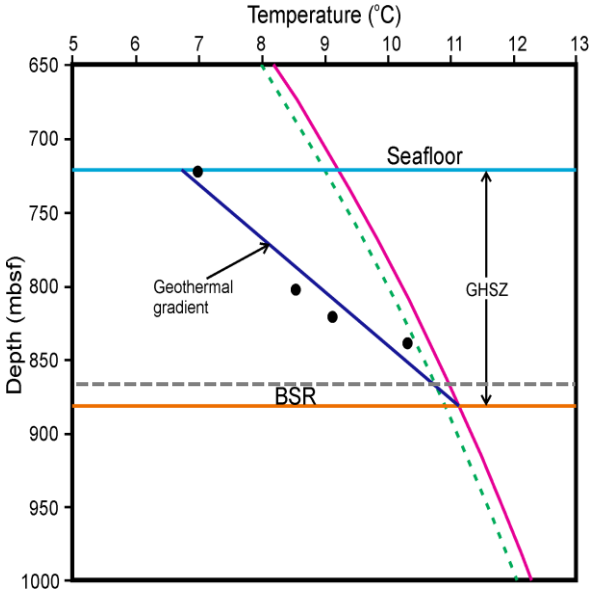

Figure 4: Base of gas hydrate stability zone (BGHSZ) phase boundarie modeling with 100% methane and 3% NaCl (pink solid line) shows BGHSZ at depth ~160 m and 3.5% NaCl (dotted green line) indicate BGHSZ depth at ~147 m in the gas hydrate drilling site. Black dots show the in situ temperature measurements and its linear fit gives the geothermal gradient ~40 °C/km.

Model-based inversion can be used for post-stack acoustic impedance inversion of seismic data, which ignores the effect of the seismic wavelet, and treats the trace as a set of reflection coefficients, with the low-frequency component added from the well logs. The advantage of this technique is its simplicity, short computation time, and robustness in the presence of noise, but thin layer interference is not accounted for since the wavelet is ignored. Sparse-spike inversion models the reflectivity as a minimal series of spikes, with spikes being added until the trace is matched accurately enough. Model-based inversion (Russell and Hampson, 1991) uses a generalized linear inversion algorithm, which attempts to modify the initial model until the resulting synthetic matches the seismic trace within some acceptable bounds. This method is effective when there is considerable knowledge about the geology and a reliable model can be created. We utilized the model-based inversion technique as reliable well-log or LWD data are available at the drill sites of IODP 372. An initial model for the inversion runs was generated using the P-impedance logs calculated at the well locations.

Acoustic impedance inversion and porosity inversion

After inversion analysis at well location, the inverted impedance obtained along seismic line. High impedance was observed above base of gas hydrate stability zone impedance was observed below BSR, probable free gas zone. A small patch of high acoustic impedance was observed just above the base of landslide debris may be due to coarse grain sand deposition (fig. 5).

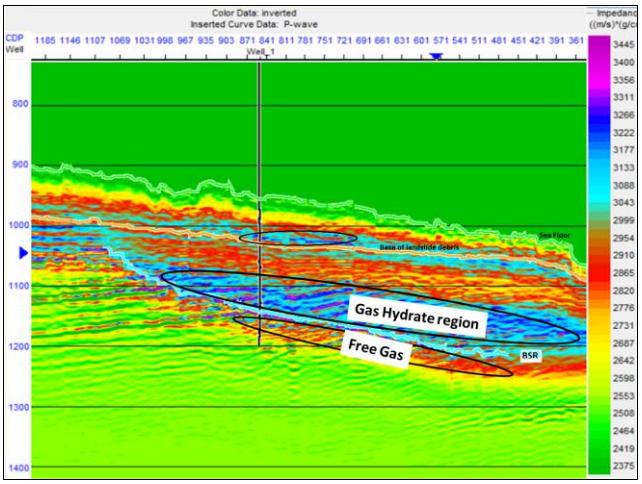

Figure 5: Inverted acoustic impedance along the seismic line showing high impedance and low impedance values respectively at gas hydrates and free gas zone and small patch of high impedance just above bas of landslide debris.

The inverted porosity along seismic line obtained from porosity inversion shown in figure 6. Low porosity above BSR in gas hydrate zone and high porosity in the free gas zone below BSR was observed on seismic section. Low to medium acoustic impedance and medium to high porosity below seafloor was observed due to presence of unconsolidated clay/silt sediments.

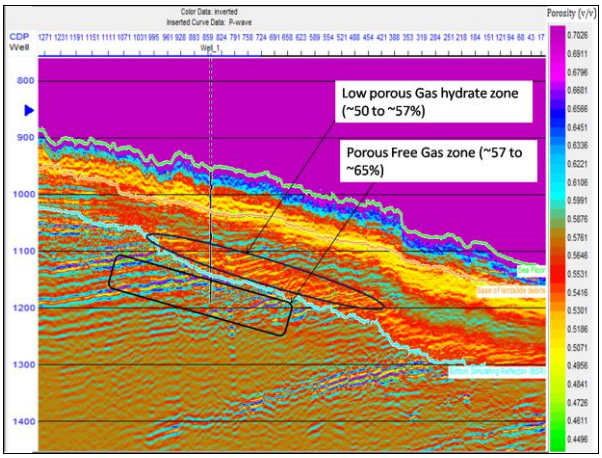

Figure 6: Inverted porosity along the seismic line showing low porosity in gas hydrate zone above BSR and high porosity below BSR in free gas zone.

Conclusions

Estimation of Acoustic impedance and porosity implemented on seismic section using model based acoustic impedance inversion and porosity inversion. The acoustic impedance and porosity wavelet inversely correlated due to negative trend between acoustic impedance and porosity. The porosity wavelet is convolved with porosity reflectivity and a better correlation is achieved between resulting synthetic and seismic traces. This work demonstrated porosity prediction methodology from post-stack seismic data. Predicted porosity section is following a good correlation with the geological trends of Hikurangi margin. The inverted acoustic impedance and porosity varies from 3050 to 3450 m/s*g/cc and 50% to 60% respectively in gas hydrate bearing zone whereas low value of acoustic impedance about 2600 to 3000 m/s*g/c and high porosity value in the range of 60-70% corresponds to occurrence of free gas.

References

Helgerud, M.B., Dvorkin, J., Nur, A., 1999, Elastic-wave velocity in marine sediments with gas hydrates: Effective medium modeling; Geophysical Research Letters, 26, 2021-2024.

Hyndman, R.D., Spence, G.D., Chapman, N.R., Riedel, M., Edwards, R.N., 2001, Geophysical Studies of Marine Gas Hydrate in Northern Cascadia, in Paull C.K., Dillon, W.P., (Eds.), Natural gas

hydrates: occurrence, distribution, detection; American Geophysical Union Monographs, 124, 273-295.

Kumar, R., Das, B., Chatterjee, R., Sain, K, 2016, A methodology of porosity estimation from inversion of post-stack seismic data; Journal of Natural Gas Science and Engineering, 28, 356-364

Pecher, I.A., Barnes, P.M., LeVay, L.J., and the Expedition 372 Scientists, 2018, Expedition 372 Preliminary Report: Creeping Gas Hydrate Slides and Hikurangi LWD. International Ocean Discovery Program. https://doi.org/10.14379/iodp.pr.372.2018

Rasmussen, K.B., Maver, K.G., 1996. Direct inversion for porosity of post stack seismic data; In: European 3-D Reservoir Modeling Conference, Stavanger. Society of Petroleum Engineers paper id: SPE 35509.

Shankar, U., Riedel, M., 2010, Seismic and heat flow constraints from the Krishna-Godavari Basin gas hydrate system; Marine Geology, 276, 1-13.

Shankar, U., Riedel, M., 2011, Gas hydrate saturation in the Krishna-Godavari basin from P-wave velocity and electrical resistivity logs; Marine and Petroleum Geology, 28, 1768-1778.

Russell, B., Hampson, D., 1991, Comparison of post stack inversion methods; In: 61st Annual International Meeting, SEG, Expanded Abstracts, 10, 876-878.

Stoll, R.D., Ewing, J.I., Bryang, M., 1971, Anomalous wave velocities in sediments containing gas hydrates; Journal of Geophysical Research - Solid Earth,76, 2090-2094.

Taylor, M.H., Dillon, W.P., Pecher, I.A., 2000, Trapping and migration of methane associated with the gas hydrate stability zone at the Blake Ridge Diapir: new insights from seismic data; Marine Geology, 164, 79-89.

Tucholke, E., Bryang, M., Ewing, J.I., 1977, Gas hydrate horizons detected in seismic-profiler data from the western North Atlantic; American Association of Petroleum Geologists Bulletin, 61, 698-707.

Acknowledgements

I would like to thank IODP Expedition 372 scientists and crew members of world different parts who acquired the log and core data used in this analysis.